The Journal of Neuroscience, May 15, 1999, *19*(10):3711–3722

A Current Activated on Depletion of Intracellular Ca^{2+} Stores Can Regulate Exocytosis in Adrenal Chromaffin Cells

Alla F. Fomina and Martha C. Nowycky

Department of Neurobiology and Anatomy, Medical College of Pennsylvania Hahnemann University, Philadelphia, Pennsylvania 19129

Exocytosis in excitable cells is strongly coupled to Ca^{2+} entry through voltage-gated channels but can be evoked by activation of membrane receptors that release Ca^{2+} from inositol 1,4,5-trisphosphate-sensitive internal stores. In many cell types, depletion of Ca^{2+} stores activates Ca^{2+} influx across the plasma membrane, a process known as capacitative or store-operated Ca^{2+} entry. This influx is mediated by a number of voltage-independent, Ca^{2+}-selective currents. In addition to replenishing Ca^{2+} stores, these currents are hypothesized to play an important role in agonist-evoked secretion in nonexcitable cells, although this has not been confirmed experimentally. The existence and physiological function of such currents in excitable cells is not known. Using the capacitance detection technique to monitor exocytosis, we provide direct experimental evidence that a similar mechanism exists in bovine adrenal chromaffin cells. Depletion of intracellular Ca^{2+} stores with thapsigargin, a SERCA pump inhibitor, or with BAPTA, an exogenous Ca^{2+} chelator, activates a small-amplitude, voltage-independent current that is carried by Ca^{2+} and Na^{+} ions. Ca^{2+} entry through this pathway is sufficient to stimulate exocytosis at negative membrane potentials. In addition, depolarization-evoked exocytosis is markedly facilitated on activation of the current. These data suggest that excitable cells possess a store-operated Ca^{2+} influx mechanism that may both directly trigger exocytosis and modulate excitation–secretion coupling.

Key words: exocytosis; calcium-secretion coupling; store-operated current; capacitance detection; synaptic plasticity; chromaffin cell, capacitative Ca^{2+} entry

Exocytosis of neurotransmitters, neuroactive peptides, and hormones at synapses and in excitable secretory cells is triggered by elevation of intracellular Ca^{2+} ($[Ca^{2+}]_i$) (Katz, 1962; Douglas and Rubin, 1963). Opening of voltage-gated Ca^{2+} channels constitutes the major pathway for rapid Ca^{2+} influx in excitable cells (Augustine et al., 1987). However, alternative pathways can contribute to Ca^{2+} elevation, such as Ca^{2+} influx through ligand-gated ion channels (Mollard et al., 1995; Gray et al., 1996) or Ca^{2+} release from intracellular stores (Berridge, 1998). The relative significance and interactions among these Ca^{2+} sources are not well understood.

Adrenal chromaffin cells are developmentally related to sympathetic neurons, and their main function is the synthesis, storage, and release of catecholamines. Exocytosis of catecholamine-containing large dense-cored vesicles is evoked by Ca^{2+} entry through voltage-gated channels, but also can be triggered by stimulation of membrane receptors coupled to inositol 1,4,5-trisphosphate (IP_3) formation and Ca^{2+} release from intracellular stores (Burgoyne, 1991). In voltage-clamped chromaffin cells, exocytosis can be evoked in the absence of depolarization by photolysis of caged IP_3 (Robinson et al., 1996) or by stimulation of membrane receptors with bradykinin (Augustine and Neher, 1992).

In many cell types, $[Ca^{2+}]_i$ elevation in response to IP_3-generating agonists is biphasic: an initial transient rise caused by Ca^{2+} release from stores is followed by a second prolonged phase that requires extracellular Ca^{2+} influx (Berridge, 1995). In some excitable cells, the prolonged phase can be at least partially supported by increased activity of voltage-gated Ca^{2+} channels (Fomina and Levitan, 1995; Li et al., 1997). In nonexcitable cells, partial or complete depletion of intracellular Ca^{2+} stores activates voltage-independent Ca^{2+} influx ("capacitative Ca^{2+} entry") (Putney, 1986, 1990).

Although the signal generated by store-depletion remains elusive, progress has been made in characterizing capacitative Ca^{2+} influx in nonexcitable cells. The best-studied mechanism is the Ca^{2+} release-activated Ca^{2+} current (I_{CRAC}) found in mast cells, lymphocytes, and leukemia cells (Penner et al., 1988; Lewis and Cahalan, 1989; Hoth and Penner, 1992, 1993). I_{CRAC} is a small-amplitude, highly Ca^{2+}-selective current that is activated by various agents that deplete intracellular Ca^{2+} stores, including inhibitors of endoplasmic reticulum Ca^{2+}/ATPases (SERCA pumps) and high concentrations of Ca^{2+} chelators (Fasolato et al., 1994; Parekh and Penner, 1997). Several other currents activated on store depletion have been described in nonexcitable cells that differ from I_{CRAC} in certain biophysical properties, such as ion selectivity or kinetics. Collectively, such currents are called "store-operated currents" (SOCs) (Clapham, 1995). The existence of capacitative Ca^{2+} entry in secretory excitable cells, including chromaffin, pituitary, and pancreatic β-cells, has been suggested, but the underlying mechanisms have not been characterized (Robinson et al., 1992: Villalobos and Garcia-Sancho, 1995; Powis et al., 1996; Liu and Gylfe, 1997).

Received Dec. 1, 1998; revised March 2, 1999; accepted March 4, 1999.

This work was supported by Grant NS22281 from the National Institute of Neurological Diseases and Stroke. We thank Drs. N. I. Chernevskaya, K. L. Engisch, and R. Nichols for comments on this manuscript, Dr. M. Cahalan for reading an earlier version of this manuscript, A. Dromaretsky for technical assistance and computer programming, and Irina Chernysh for immunohistochemistry.

Correspondence should be addressed to Dr. Martha C. Nowycky, Department of Pharmacology and Physiology, University of Medicine and Dentistry of New Jersey, 185 South Orange Avenue, Newark, NJ 07103.

Dr. Fomina's present address: Department of Physiology and Biophysics, University of California, Irvine, CA 92697.

In addition to replenishing intracellular Ca^{2+} stores, SOCs play a critical role in gene expression in nonexcitable cells (Fanger et al., 1995; Dolmetsch et al., 1998). It has also been proposed, although not demonstrated directly, that Ca^{2+} influx through SOCs is a central element in agonist-evoked secretion in mast cells (Zhang and McCloskey, 1995). However, in mast cells, Ca^{2+} is merely a cofactor for secretion, and Ca^{2+} elevation is not strictly required (Neher, 1988). Thus, the significance of SOCs in secretion in nonexcitable cells remains unclear. In excitable cells, in which the secretory machinery is highly sensitive to Ca^{2+}, the role of SOCs has not been studied. Here, we examine the existence, properties, and functional significance of a SOC in adrenal chromaffin cells.

MATERIALS AND METHODS

Electrical recording techniques

Bovine adrenal chromaffin cells were cultured as described previously (Vitale et al., 1991; Engisch and Nowycky, 1996). Most recordings were performed with perforated-patch voltage-clamp techniques using an Axopatch 200A amplifier (Axon Instruments, Foster City, CA) and programs written in Axobasic (Axon Instruments, Foster City, CA). Experiments were performed at 30°C.

Recording protocols. Time was set to zero on seal formation, and data acquisition during perforated-patch experiments was initiated after 5–10 min when the series resistance stabilized at 6–15 MΩ. The initial cell capacitance ranged from 4 to 8 pF. Exocytosis was monitored as changes in membrane capacitance (C_m) using a computer-based phase-detection technique as described previously (Lim et al., 1990; Seward et al., 1995). The membrane potential was held at −90 mV; C_m and combined membrane and series conductance (G) values were calculated from sets of 10 sine waves, 1.2 kHz, 15 mV root mean square. The sets were separated by ~2 msec for data calculation and storage, resulting in a final temporal resolution of ~12 msec per data point. Capacitance data were acquired in 11.8 sec segments; the C_m and G phase angles were reset at the beginning of each segment. The holding current (I_{hold}) was measured at −90 mV between sets of sine waves. Five measurements of I_{hold} at 160 msec intervals were obtained every 11.8 sec. In some experiments, voltage ramp pulses (−120 to −60 mV, 200 msec duration) were applied every 11.8 sec. In the figures, the current is shown over the range of −115 to −60 mV to exclude the capacitative transient. Voltage-gated Ca^{2+} entry was evoked by single brief depolarizing pulses (−90 mV to −10 or +10 mV; 20–80 msec duration) that were administered once every 1–4 min.

Data analysis. For calculation of the rate of depolarization-independent C_m changes, 200–1000 points of a C_m trace were averaged, and the resulting plot was then differentiated. Depolarization-evoked exocytosis was calculated as the difference in C_m value before and after depolarization by averaging 3 C_m data points. The amount of Ca^{2+} influx during depolarization was calculated by integration of voltage-gated Ca^{2+} currents using limits that excluded the voltage-gated Na^+ current and is expressed in charge units (Q_{Ca}). Tetrodotoxin (TTX) was not used, because Na^+ channels in bovine chromaffin cells are relatively insensitive to TTX, and TTX contributes a capacitative artifact attributable to slowing of Na^+ channel gating current (Horrigan and Bookman, 1994). Holding current is presented as the five-point average and SEM of current samples obtained at 160 msec intervals within an 11.8 sec segment.

Data analysis was performed with Axobasic programs and Origin 4.1 (Microcal, Northhampton, MA) software. All statistics are presented as mean ± SEM. The number of experiments reported in the text varies somewhat, because not all parameters (F_{Ca}, I_{Tg}, and ΔC_m) could be successfully measured in all cells. Early experiments did not monitor I_{hold} but are included in statistics for changes in F_{Ca} and ΔC_m.

Solutions

Extracellular recording solutions. The recording solutions consisted of the following (in mM): (1) standard solution: 55 NaCl, 70 NaOH, 5 $Ca(OH)_2$, 0.8 $MgCl_2$, 20 TEA-OH, 10 HEPES, 10 glucose; (2) low Ca^{2+} solution: 55 NaCl, 70 NaOH, 0.5 or 1.0 $Ca(OH)_2$, 5 $MgCl_2$, 20 TEA-OH, 10 HEPES, 10 glucose; (3) low Cl^- solution: standard solution with 10 NaCl, 115 NaOH. The pH of external solutions 1–3 was adjusted to 7.35 with methanesulfonic acid; and (4) nominally Na^+-free solution: standard solution with equimolar replacement of Na^+ with *N*-methyl-D-glucamine ($NMDG^+$), pH adjusted to 7.35 with HCl.

Pipette solutions. (1)For perforated-patch experiments, the solution consisted of the following (in mM): 130 Cs-glutamate, 10 CsCl, 5 $MgCl_2$, 10 Na-HEPES, pH adjusted to 7.2 with CsOH (ICN, Aurora, OH). Amphotericin B (Calbiochem, La Jolla, CA) at a final concentration of 0.4–0.5 mg/ml (stock solution in DMSO: 125 mg/ml) was used for perforation. (2) For whole-cell recordings, the solution consisted of the following (in mM): 130 Cs-glutamate, 2 Mg-ATP, 10 HEPES, 9.5 NaCl, 10 BAPTA, pH adjusted to 7.2 with CsOH.

Thapsigargin (Tg) (Calbiochem, La Jolla, CA) was stored at −20°C for up to 1 month as a 10 mM stock solution in DMSO. Recording solutions and drugs were applied using a perfusion pipette with a tip diameter of ~50 μm placed ~50 μm from the cell. Five barrels were inserted close to the pipette tip, and solution exchange was controlled by manual valves. A complete exchange of solution in the vicinity of the patched cell was achieved within 5 sec.

Unless otherwise noted, all compounds were from Sigma (St. Louis, MO).

Measurement of Ca^{2+}-sensitive dye fluorescence

For perforated-patch experiments, cells were preloaded with the ester forms of nonratiometric (Oregon Green 488 BAPTA-1/AM or Fluo-3 AM; Molecular Probes, Eugene, OR) or ratiometric (fura-2 AM; Molecular Probes) Ca^{2+}-sensitive fluorescent dyes. The dye-loading solution contained (in mM): 150 NaCl, 1.8 $CaCl_2$, 0.8 $MgCl_2$, 2.5 KCl, 10 Na-HEPES, 10 glucose, pH 7.3. The culture media was replaced with loading solution containing 2.5 μl/ml of Oregon Green 488 BAPTA-1/AM or Fluo-3 AM stock (0.8 mM in DMSO) or 1 μl/ml of fura-2 AM stock (1.5 mM in DMSO) and 5 μl/ml of 10% Pluronic F-127 solution in DMSO. Cells were incubated with the dye-containing solution for 10–30 min at 37°C, washed, and then held in the loading solution for at least 30 min at 37°C to allow cleavage of the acetoxymethyl ester. Fluorescence images of nonratiometric dyes were acquired with the Bio-Rad MRC-600 laser scanning confocal imaging system (Bio-Rad, Hercules, CA) using single wavelength excitation (488 nm line of argon-krypton laser) and a 520 nm long-pass barrier filter and were processed off-line with NIH Image analysis software. Unless indicated otherwise, the image sampling interval was 700 msec during and immediately after depolarizing pulses and 10 sec at other times. Changes in intracellular Ca^{2+} are expressed as fluorescence intensity (F) normalized to the value at the beginning of the experiment (F_0). Fura-2 fluorescence was monitored using the Multipoint Imaging Photometer system (Dromaretsky et al., 1997) with signal acquisition at 360/380 nm excitation wavelengths every sec. For fura-2 experiments the ratio F_{360}/F_{380} is presented.

Dopamine-β-hydroxylase immunocytochemistry and confocal microscopy

Cells were washed in normal recording solution and incubated for 2 min at 37°C in the standard recording solution containing 5 μM Tg or vehicle alone (control). After rinsing three times with PBS, PBS was replaced with fixative (4% paraformaldehyde/0.4% saponin in PBS, pH 7.4) for 10 min at room temperature. Fixed cells were washed three times with PBS and then incubated for 20 min with 10% goat serum (Jackson ImmunoResearch Laboratories, West Grove, PA) to reduce nonspecific staining. After rinsing, cells were labeled with a 1:1000 dilution of polyclonal anti-dopamine-β-hydroxylase (DβH) antibodies (Chemicon, Temecula, CA) for 1 hr and rinsed again with PBS containing 10% goat serum. Cells were incubated with goat anti-rabbit IgG FITC-conjugated secondary antibodies (1:200, Jackson ImmunoResearch Laboratories) for 1 hr. Nonspecific fluorescence was assessed by incubating cells with the secondary fluorescent antibodies only. After fluorescent labeling, cells were rinsed three times with 10% goat serum and PBS, preserved under 4% *p*-phenylenediamine in glycerol, and stored at −20°C until examination.

Immunofluorescent staining was visualized with a Bio-Rad MRC-600 laser scanning confocal imaging system (see above) with a 63× oil objective (numerical aperture 1.4). Single confocal sections were taken with pin-hole aperture settings of 2 at the plane of maximal nuclear diameter. FITC emission was excited using the argon laser 488 nm line and filtered with a 520 nm long-pass barrier filter. Images of randomly selected cells from stimulated and control groups were recorded at the same settings, and the average fluorescence intensity value was measured.

RESULTS

To investigate the presence and potential physiological role of a capacitative Ca^{2+} entry pathway in adrenal chromaffin cells, we combined voltage clamp and fluorometric techniques to monitor simultaneously membrane conductance, intracellular Ca^{2+} ($[Ca^{2+}]_i$), and exocytosis in single bovine chromaffin cells. To preserve essential cytoplasmic regulatory elements, most experiments were performed using the perforated-patch-clamp method (Rae et al., 1991) at elevated temperature (~30°C). Changes in $[Ca^{2+}]_i$ were monitored by measuring the fluorescence of a Ca^{2+}-sensitive dye preloaded into the cells (F_{Ca}). Exocytosis was assayed with a software-based capacitance detection technique as changes in cell surface area (ΔC_m) (Neher and Marty, 1982; Joshi and Fernandez, 1988; Fidler and Fernandez, 1989). Intracellular Ca^{2+} stores were depleted with Tg, which inhibits SERCA pumps and thereby prevents the reuptake of cytoplasmic Ca^{2+} passively released from the stores in many cell types, including bovine chromaffin cells (Thastrup et al., 1990; Robinson and Burgoyne, 1991; Zerbes et al., 1998).

Thapsigargin-induced changes in membrane conductance, intracellular Ca^{2+}, and exocytosis

Tg application (1–5 μM) activated a relatively small amplitude inward current at negative holding potentials (Fig. 1*A*, I_{hold}) and produced a rise in F_{Ca} (Fig. 1*A*, F/F_0) in 23 of 31 cells. The onset of the Tg-activated current (I_{Tg}) and the rise in F_{Ca} were simultaneous within the limits of our experimental resolution (~10 sec) and usually began 1–2 min after Tg application (Fig. 1*C*). I_{Tg} often had complex kinetics with periodic partial declines in amplitude. These slow current oscillations were correlated with oscillations in the F_{Ca} signal. I_{Tg} reached a maximal value after several minutes that, on average, was −15.2 ± 2.7 pA at −90 mV (n = 18; here and elsewhere, n = number of cells where the parameter of interest could be accurately measured). I_{Tg} inactivated fully in the continuous presence of Tg, returning to the prestimulatory level within several minutes; F_{Ca} declined with a similar time course. Subsequent application of higher doses of Tg resulted in reactivation of I_{Tg} and produced an additional rise in F_{Ca} (data not shown). Voltage-gated Ca^{2+} currents that evoked large-amplitude F_{Ca} transients (Fig. 1*A–C*, *vertical bars*) never elicited I_{Tg}-like inward currents either before or after Tg application, suggesting that I_{Tg} is not activated by a rise in $[Ca^{2+}]_i$.

In all cells with a Tg-induced rise in F_{Ca}, the cell surface area increased in the absence of voltage-gated Ca^{2+} entry (Fig. 1*A,C*, ΔC_m) (n = 23). The onset of the C_m increase was clearly delayed relative to the onset of I_{Tg} and rise in F_{Ca} (42.9 ± 8.32 sec; n = 18) (Fig. 1*C*; also see Fig. 4*B*). Depolarization-independent exocytosis proceeded at a slow rate (17.3 ± 4.3 fF/sec, n = 16) but was substantial (930.1 ± 187.9 fF, n = 10, compare with 4–8 pF initial cell capacitance). The C_m increase often terminated before the decline of F_{Ca} and I_{Tg}, and the total ΔC_m increase may be underestimated because of contaminating endocytosis. The occurrence and kinetics of endocytosis were variable, had no obvious correlation with changes in I_{Tg} or F_{Ca}, and were not analyzed further.

In a subset of experiments, I_{Tg} was activated without a concurrent rise in global F_{Ca} (Fig. 1*B*) (8 of 31 cells at [Tg] from 1 to 5 μM and 4 of 11 cells at [Tg] from 0.1 to 1 μM). In these cells, I_{Tg} was smaller, with a maximal current increase over control levels of ~5 pA. The kinetics were more complex as the current periodically decayed to the prestimulatory levels, but current oscillations persisted for the duration of the experiment (Fig. 1*B*, I_{hold}). Depolarization-independent exocytosis was never detected when Tg application failed to evoke a global F_{Ca} rise (n = 12 of 12). In these cells, C_m increases were detected only in response to depolarizations that activated voltage-gated Ca^{2+} channels (Fig. 1*B*).

Exocytosis evoked by voltage-gated Ca^{2+} entry was potently enhanced in all cells in which I_{Tg} was activated (Fig. 2) (n = 35). In control conditions, changes in C_m evoked by brief depolarizations (20–80 msec) were small (10–50 fF) (Fig. 2*A,B*; same cells as in Fig. 1*A,B*, respectively), and the relationship between ΔC_m and the amount of voltage-gated Ca^{2+} influx (Q_{Ca}) was satisfactorily described by a linear function over this restricted range of stimulus parameters (Fig. 2*C,D*). After Tg application, ΔC_m responses were enhanced, despite a reduction in the amplitude of voltage-gated Ca^{2+} currents (Fig. 2*A,B*). The facilitated responses were substantially larger than predicted by the linear $\Delta C_m/Q_{Ca}$ relationship (Fig. 2*C,D*). Facilitation had a different time course and magnitude in cells with (Figs. 1*A*, 2*A*) and without (Figs. 1*B*, 2*B*) a detectable rise in F_{Ca}. In cells with an F_{Ca} rise, both I_{Tg} and facilitation were transient, subsiding by 9–12 min (Fig. 2*E*). Before Tg application, the Ca^{2+} efficacy ($\Delta C_m/Q_{Ca}$) was ~1.5 fF/pC. Maximal facilitation occurred at ~3 min, where the average $\Delta C_m/Q_{Ca}$ value was >10 fF/pC. In cells without a detectable F_{Ca} rise, both I_{Tg} and facilitation were sustained even at 20 min after Tg application (Fig. 2*F*). The average maximal efficacy of ~4 fF/pC was reached after ~5–6 min. Thus, in both groups of cells, the time course of facilitation corresponded to that of I_{Tg}, and the magnitude of facilitation was approximately proportional to the current amplitude.

Mechanisms underlying thapsigargin-induced modulation of exocytosis

We consistently observed depolarization-independent exocytosis in all cells in which global $[Ca^{2+}]_i$ was elevated by Tg application. The lack of an F_{Ca} rise in cells with a small amplitude I_{Tg} might indicate that Tg-induced Ca^{2+} discharge from the stores and/or Ca^{2+} influx are compensated by other uptake, extrusion, or buffering systems. Facilitation of depolarization-evoked exocytosis in these cells, however, suggests that local, submembrane Ca^{2+} changes may occur even in the absence of a detectable F_{Ca} rise. We tested whether the major source of Ca^{2+} underlying the F_{Ca} rise and the depolarization-independent exocytotic response was intracellular or extracellular.

To examine the contribution of Ca^{2+} released from intracellular stores, Tg was applied in external solutions containing low Ca^{2+}. Exchange to a nominally Ca^{2+}-free external solution (no added Ca^{2+}) caused the appearance of a large-amplitude, inward current. This resembled a current described by Armstrong and Lopez-Barneo (1987) in squid neurons that is thought to arise from the loss of gating and selectivity of voltage-gated ion channels in Ca^{2+}-free solution. Low concentrations of Ca^{2+} prevented the appearance of this current and were used in all further perforated-patch experiments.

Exchange from normal (5 mM) to low Ca^{2+} (0.5 mM) external solution resulted in a rapid decline in the F_{Ca} signal (data not shown). This is probably attributable to a combination of a decrease in the driving force for Ca^{2+} entry through leak channels (Obejero-Paz et al., 1998) and the activity of a number of Ca^{2+} extrusion mechanisms, including the Na–Ca exchanger and plasma membrane Ca^{2+} pump (Chern et al., 1992). When cells were exposed to a low Ca^{2+} solution containing high doses of Tg (5–14 μM), there was an initial decline in the F_{Ca} signal, followed by a delayed, slow rise in F_{Ca} that did not reach levels recorded

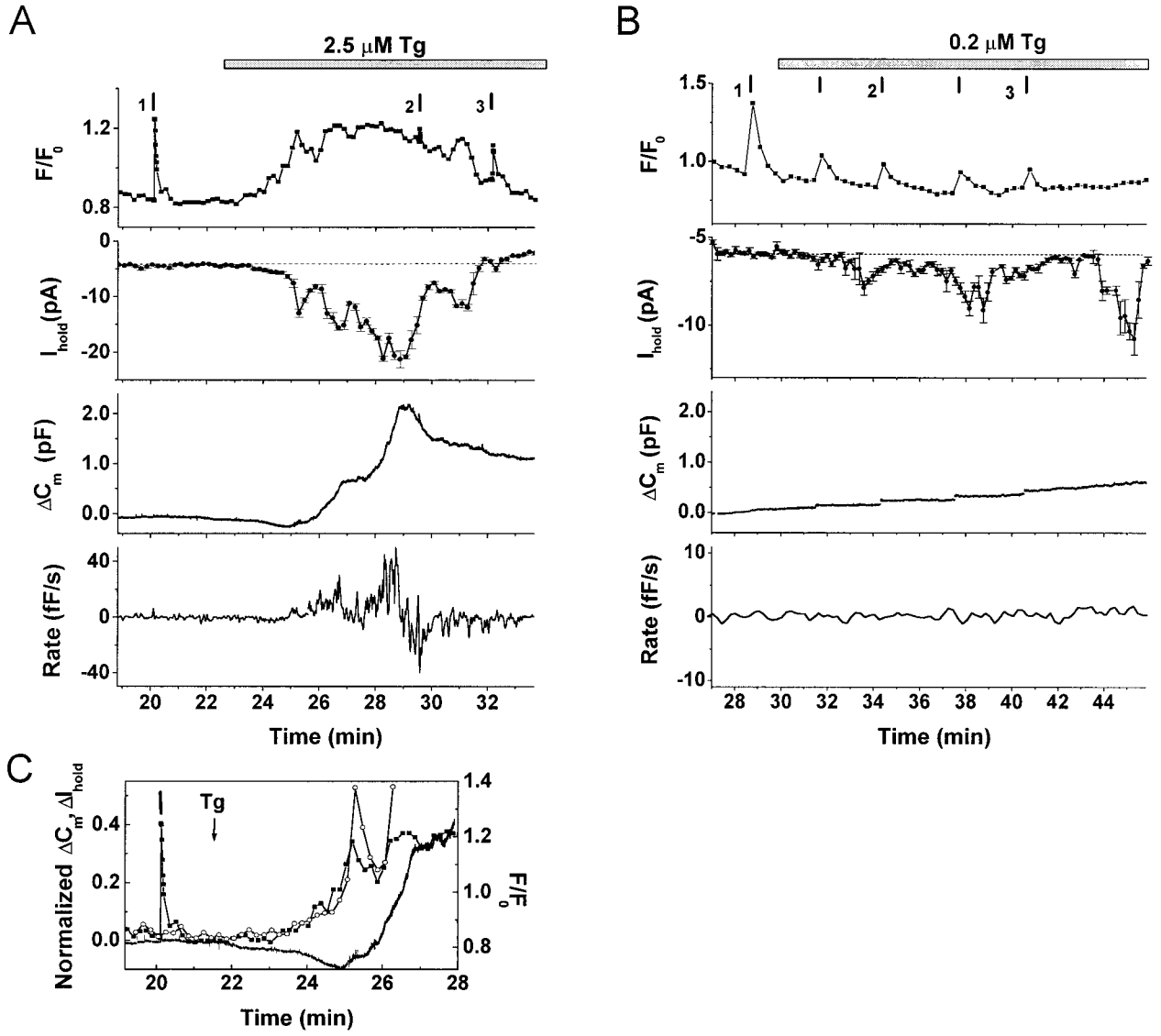

Figure 1. Effects of thapsigargin on intracellular $[Ca^{2+}]$, membrane conductance, and exocytosis. Simultaneous recordings in individual cells of Ca^{2+}-sensitive dye fluorescence (F_{Ca}), current at −90 mV (I_{hold}), and changes in membrane capacitance (ΔC_m). *Vertical bars* indicate timing of depolarizing pulses. In standard recording solution, brief depolarizations evoked voltage-gated Ca^{2+} currents, rapid F_{Ca} transients, and abrupt increases in C_m (also see Fig. 2*A,B*) that reflect exocytosis of catecholamine-containing large dense-cored vesicles (Chow et al., 1992; Engisch and Nowycky, 1998). *A*, Tg application induced a rise in F_{Ca} (F/F_0), activated a transient inward current (I_{hold}), and evoked depolarization-independent exocytosis (ΔC_m). The *bottom panel* is the calculated rate of depolarization-independent exocytosis (*Rate*). Tg (2.5 μM) was applied continuously as indicated. Fluorescent dye: Oregon Green BAPTA-1 AM. *B*, Tg application activated an inward current that was not accompanied by changes in F_{Ca} or depolarization-independent exocytosis (ΔC_m). Panels as in *A*. Tg (0.2 μM Tg) was applied as indicated. Slow C_m drifts (maximal rate <1 fF/sec) were often observed during prolonged recording (Engisch and Nowycky, 1998) but had no consistent correlation with Tg application. In this particular experiment, the fluorescence signal was sampled every 20 sec; therefore, the F_{Ca} responses to depolarizations are truncated. Fluorescent dye: Fluo-3 AM. *C*, *Superimposed traces* from 1*A* of F_{Ca} (■), I_{hold} on a reversed axis (○), and ΔC_m (*line*) on an expanded time scale. C_m and I_{hold} values were normalized to the maximal values after Tg application and are presented on the same scale. The F_{Ca} trace was scaled to match the time course of the initial rise of I_{Tg}.

before solution exchange (Fig. 3). The small rise in F_{Ca} probably reflects Ca^{2+} accumulation after block of Ca^{2+} reuptake by Tg. However, it was not associated with detectable activation of I_{Tg} or a significant increase in C_m. Thus, under our experimental conditions, passive discharge from intracellular stores is not sufficient to elevate $[Ca^{2+}]_i$ above control levels or to initiate depolarization-independent exocytosis, even in the presence of very high concentrations of Tg.

If the F_{Ca} rise and exocytotic responses are caused by extracellular Ca^{2+} entry, I_{Tg} may be the Ca^{2+}-carrying current. In this case, pharmacological block of I_{Tg} or lowering of extracellular Ca^{2+} should inhibit $[Ca^{2+}]_i$ elevation and exocytosis. To test this hypothesis, we varied the composition of the external solution after activation of I_{Tg} in normal recording solution. Only cells that responded to Tg with a detectable rise in F_{Ca} were included in the analysis.

Zn^{2+} is an inorganic blocker of SOCs in mast cells and other nonexcitable cells (Hoth and Penner, 1993; Zhang and McCloskey, 1995), but it has little direct effect on the exocytotic mechanisms of permeabilized bovine chromaffin cells when applied at

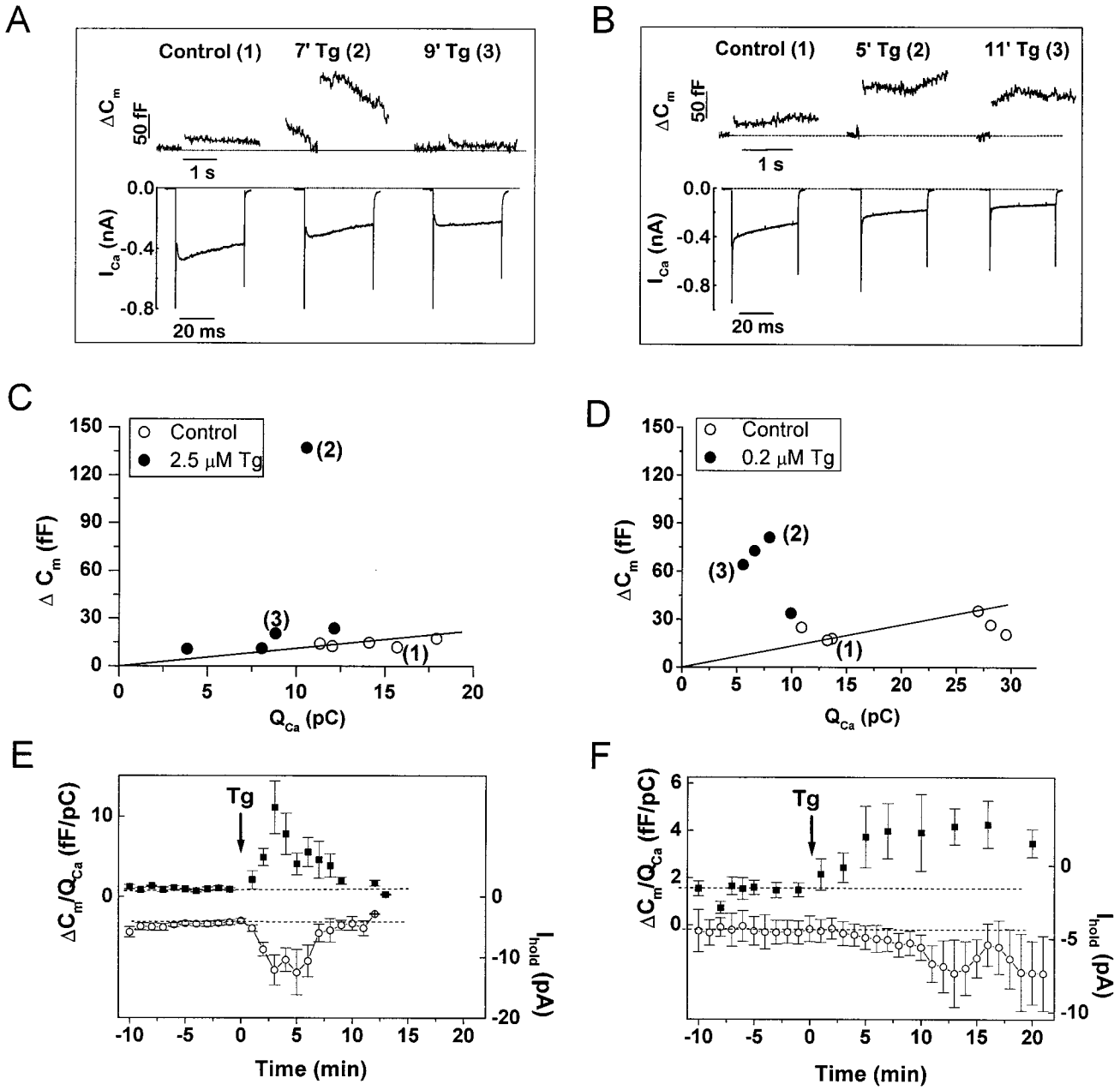

Figure 2. Facilitation of depolarization-evoked exocytosis by thapsigargin. *A*, *B*, Capacitance changes (ΔC_m, *top traces*) and corresponding voltage-gated Ca^{2+} currents (I_{Ca}, *bottom traces*) evoked by depolarizations before and after application of Tg (2.5 μM in *A*; 0.2 μM in *B*) on an expanded time scale. Data from the same cells as in Figure 1 *A,B*. *Numbers in parentheses* above the C_m traces indicate the corresponding depolarizations in Figure 1, *A* and *B*, respectively. *C*, *D*, Relationship between the depolarization-evoked Ca^{2+} influx expressed in charge units (Q_{Ca}) and corresponding capacitance changes (ΔC_m) before (○) and after (●) application of 2.5 μM [*C(3)*] or 0.2 μM (*D*) Tg. Single depolarizations to +10 and −10 mV, 40 msec duration, separated by 3–4 min intervals, were given before Tg to establish the $\Delta C_m/Q_{Ca}$ relationship in control conditions. The *straight line* is the linear regression fit for control data obtained by minimizing χ^2. After Tg application all depolarizations were to +10 mV, 40 msec duration. The reduced Q_{Ca} values are caused by inhibition of voltage-gated Ca^{2+} currents by Tg. Similar reduction of amplitude of voltage-gated Ca^{2+} currents has been described previously for other cell types (Nelson et al., 1994; Buryi et al., 1995). *E*, *F*, Averaged time courses of Tg-induced changes in $\Delta C_m/Q_{Ca}$ values (■) and I_{Tg} (○). *E*, Data from 14 cells in which Tg application produced a rise in F_{Ca} and triggered depolarization-independent exocytosis. *F*, Data from 12 cells in which Tg evoked an inward current but did not cause a detectable rise in F_{Ca} and did not trigger depolarization-independent exocytosis. $\Delta C_m/Q_{Ca}$ points are the mean ± SEM values of four to six measurements from different cells that fell within a given 1 min interval. I_{hold} values were calculated by first averaging all current samples for each cell at 1 min intervals (see Materials and Methods) and then determining the mean ± SEM for all cells. In *F*, the number of experiments declined from 12 at time = 0 to 4 at time = 22 min because of the loss of gigaseals during prolonged recordings.

millimole concentrations (Tomsig and Suszkiw, 1996). All Tg-induced responses were reversibly blocked by extracellular application of Zn^{2+} (2–4 mM, $n = 8$). Figure 4*A,B* illustrates a cell with typical F_{Ca}, I_{hold}, and ΔC_m responses to Tg. On Zn^{2+} application, both I_{Tg} and depolarization-independent exocytosis ceased abruptly, whereas F_{Ca} declined more slowly (Fig. 4*A*). During voltage ramps, I_{Tg} exhibited a linear current–voltage (*I–V*) relationship between −120 and −60 mV, and Zn^{2+} blocked the current throughout this potential range (Fig. 4*C*). Return to control solutions resulted in an abrupt increase in I_{Tg}

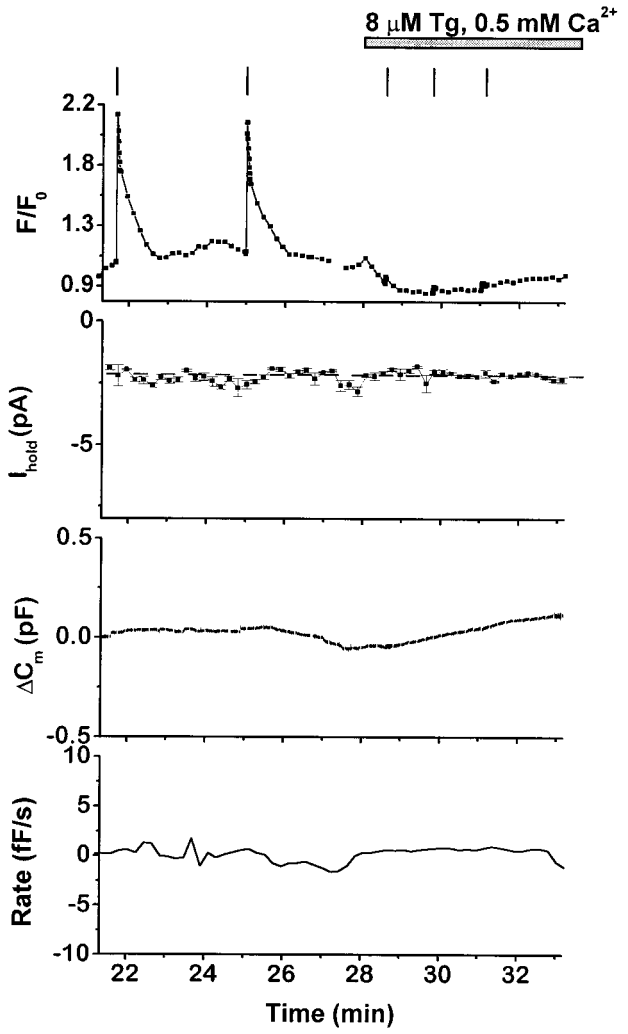

Figure 3. Effects of thapsigargin in low-Ca^{2+} external solution on intracellular $[Ca^{2+}]$, membrane conductance, and exocytosis. Simultaneous recordings of F_{Ca} (F/F_0), current at −90 mV (I_{hold}), and capacitance changes (ΔC_m) in a single cell. The *bottom panel* is the calculated rate of depolarization-independent exocytosis (*Rate*). Low-Ca^{2+} solution (0.5 mM) containing Tg (8 μM) was applied as indicated; *vertical bars* indicate timing of depolarizations. The F_{Ca} signal declined rapidly in low-Ca^{2+} solution, and depolarizations no longer produced an F_{Ca} rise or exocytosis because of the reduction of voltage-gated Ca^{2+} currents. Fluorescent dye: Oregon Green BAPTA-1 AM.

that was correlated with rapid increases in F_{Ca} and exocytosis. The amplitude of I_{Tg} after washout of Zn^{2+} was always much greater than in Tg alone (Fig. 4*A*) (−151.6 ± 24.2 pA; $n = 8$), and the current was blocked by reapplication of Zn^{2+}. The cause of I_{Tg} enhancement is not understood, but it was correlated with a substantially greater rate of exocytosis (83.5 ± 22.7 fF/sec, $n = 7$), suggesting that the rate of exocytosis may be proportional to the amplitude of I_{Tg}.

Substitution of Na^+ in the external solution with $NMDG^+$ reduced the amplitude of I_{Tg} by 58.2 ± 6% (Fig. 5*A*) ($n = 10$). This effect is clearly seen in the *I–V* relationship during a ramp from −120 to −60 mV (Fig. 5*B*) and indicates that a fraction of I_{Tg} is carried by Na^+ ions. Despite the reduced current amplitude, the F_{Ca} signal usually exhibited an additional rise in Na^+-free solution (9 of 10 substitutions). The increases in F_{Ca} are consistent with a reversal or block of the Na–Ca exchanger (Pan and Kao, 1997). In normal recording solutions, an active Na–Ca exchanger would generate an inward current at negative potentials that might contribute to I_{Tg} but would tend to lower $[Ca^{2+}]_i$. In some cells, the rate of increase of ΔC_m was slightly enhanced on exchange to Na^+-free solution. However, the effect of Na–Ca exchange on exocytosis is beyond the scope of the present study and was not pursued further.

Application of a Na^+-free, low-Ca^{2+} (0.5–1 mM) solution decreased the total inward current (not leak-subtracted) by 82 ± 6% ($n = 3$), which reduced I_{hold} to values even lower than before Tg application (Fig. 6). Simultaneously with I_{Tg} inhibition, F_{Ca} declined, and the rate of depolarization-independent exocytosis was reduced (Fig. 6). All effects were reversed on return to standard recording solution. Perfusion with low Cl^- external solution (10 mM Cl^-; see Materials and Methods) had no effect on I_{Tg}, F_{Ca}, or exocytosis ($n = 3$; data not shown), confirming that I_{Tg} is a cation-selective current.

The experiments described above (Figs. 3–6) provide strong evidence that a component of I_{Tg} is carried by extracellular Ca^{2+} and Na^+ ions and that this pathway is the major source of Ca^{2+} for elevation of $[Ca^{2+}]_i$ and depolarization-independent exocytosis in these experimental conditions. It is likely that I_{Tg} is also responsible for facilitation of depolarization-evoked exocytosis, but this could not be tested directly because voltage-gated Ca^{2+} currents were inhibited by Zn^{2+} and diminished in low-Ca^{2+} solution.

A current resembling I_{Tg} is evoked by chelating intracellular Ca^{2+} with BAPTA

The results presented so far are compatible with the hypothesis that in chromaffin cells Tg application activates a Ca^{2+}-carrying current component that may be operated by intracellular Ca^{2+} stores. To obtain additional evidence for the presence and properties of a SOC in these cells, we performed conventional whole-cell recordings with 10 mM BAPTA in the patch pipette. BAPTA depletes intracellular Ca^{2+} stores by chelating cytosolic Ca^{2+} and thereby preventing store refilling (Hoth and Penner, 1992) and has been widely used for activating SOC in various cell types (Parekh and Penner, 1997). In addition, chelation of cytosolic Ca^{2+} should minimize the activity of the Na–Ca exchanger (Chern et al., 1992).

An example of an inward current activated by intracellular perfusion with 10 mM BAPTA (I_{BAPTA}) is illustrated in Figure 7. I_{BAPTA} began to develop within 2–4 min of membrane rupture ($n = 6$ of 11 cells) and reached a maximal amplitude (−11.0 ± 1.3 pA at −90 mV; $n = 6$) within several minutes. The kinetics of activation and inactivation of I_{BAPTA} were smoother and more uniform than those of I_{Tg}, which is expected if there is less contamination by Na–Ca exchanger current. Similar to I_{Tg}, I_{BAPTA} often inactivated within several minutes and had a linear *I–V* relationship between −120 and −60 mV (Fig. 7*B*). Substitution of Na^+ in the external solution with $NMDG^+$ reduced the amplitude of I_{BAPTA} by only 26.4 ± 4.5% ($n = 6$) (Fig. 7*A,B*), consistent with the hypothesis that I_{Tg} may include both a SOC and a Na–Ca exchanger component. Removing both Ca^{2+} and Na^+ ions from the external solution reduced I_{BAPTA} by 83.5 ± 3.8% (eight solution exchanges for six cells; the large amplitude, nonspecific current did not develop when cells were perfused with the BAPTA-containing pipette solution). Application of 2 mM Zn^{2+} completely blocked I_{BAPTA} ($n = 3$; data not shown). Application of Tg to cells after I_{BAPTA} inactivation evoked an additional inward current (I_{Tg}) but had no effect on membrane

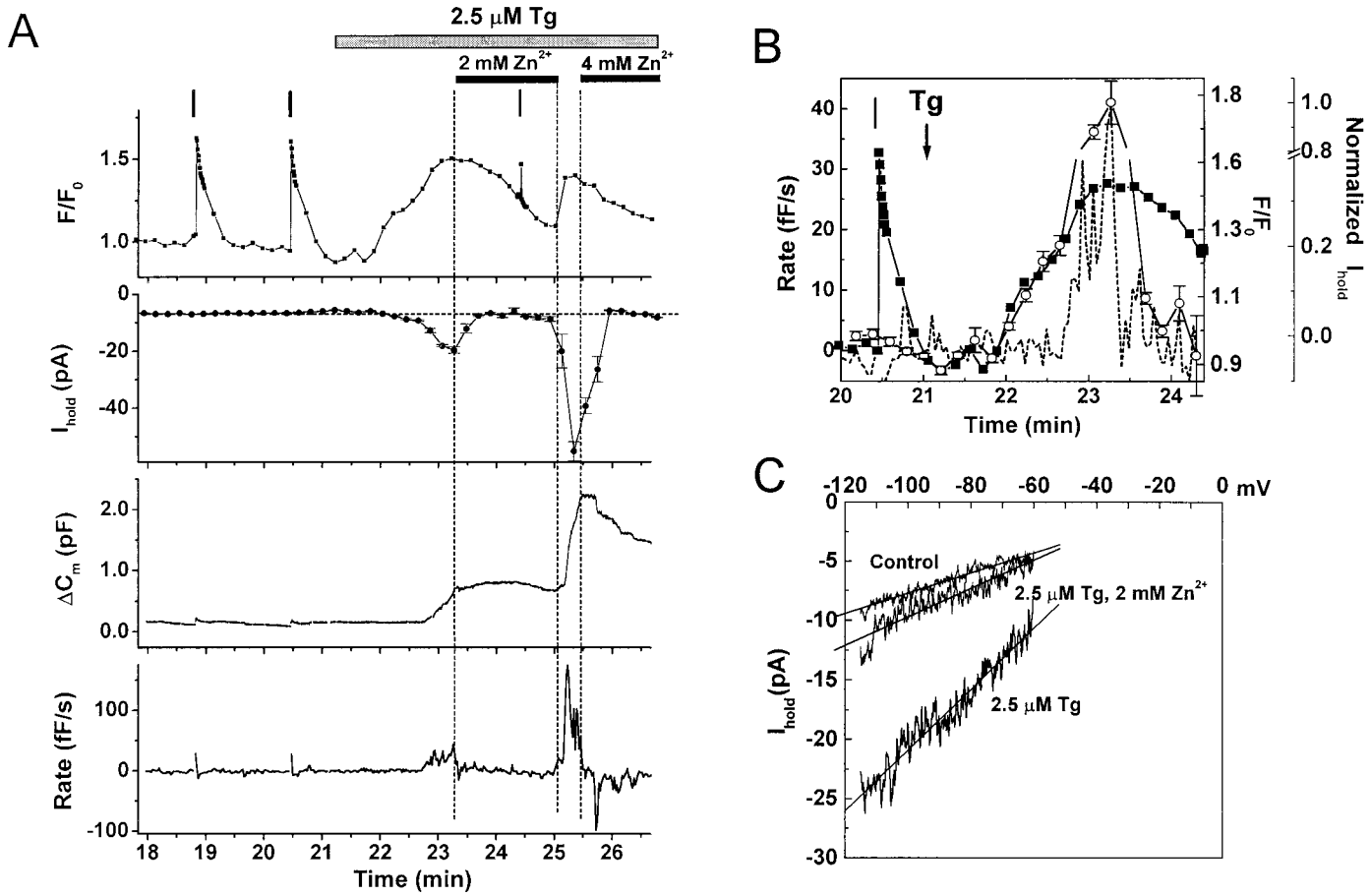

Figure 4. Inhibition by Zn^{2+} of the thapsigargin-induced increase in intracellular $[Ca^{2+}]$, inward current, and exocytosis. *A*, Simultaneous recordings of F_{Ca} (F/F_0), current at −90 mV (I_{hold}), and capacitance changes (ΔC_m) in a single cell. The *bottom panel* is the calculated rate of depolarization-independent exocytosis (*Rate*). Tg (2.5 μM) and Zn^{2+} (2 and 4 mM) were applied as indicated. *Vertical bars* indicate timing of depolarizations. Fluorescent dye: Oregon Green BAPTA-1 AM. *B*, Superimposed traces of F_{Ca} (■), I_{hold} on a reversed axis (○), and *Rate* (*dashed line*) on an expanded time scale. For scaling information, see Figure 1*C*. *C*, Currents recorded during voltage ramps from −120 to −60 mV, 200 msec duration, before Tg application (*Control*), 2 min after Tg (*2.5 μM Tg*), and 1 min after addition of 2 mM Zn^{2+} (*2.5 μM Tg, 2 mM Zn^{2+}*). Each trace is the average of three ramps. Activation of I_{Tg} was consistently associated with an increase in current noise.

capacitance ($n = 3$; data not shown), confirming that the Tg-evoked depolarization-independent exocytosis is mediated by elevation of $[Ca^{2+}]_i$.

Thapsigargin stimulates exocytosis of catecholamine-containing vesicles

The capacitance detection technique accurately reports changes in cell surface area but does not provide information on the type of membrane added. To verify that Tg stimulates exocytosis of catecholamine-containing vesicles, we labeled control and Tg-stimulated cells with antibodies against DβH and examined cells with confocal microscopy after fixation. DβH is a membrane-attached enzyme located exclusively on the inner surface of catecholamine-containing vesicles and is exposed on the cell exterior only when the vesicles undergo exocytosis (Phillips et al., 1983; Wick et al., 1997). As described above, depolarization-independent C_m increases were initiated within 1–2 min after Tg application (1–5 μM). Exposure of nonvoltage-clamped cells to 5 μM Tg for 2 min resulted in the appearance of fluorescent patches corresponding to DβH immunoreactivity on the cell surface (Fig. 8; shown in *black* in inverted images), indicating exocytosis of catecholamine-containing vesicles.

DISCUSSION

In this report, we describe a Ca^{2+}- and Na^+-carrying current activated on intracellular Ca^{2+} store depletion. Ca^{2+} influx via this pathway can provide sufficient Ca^{2+} to elevate global $[Ca^{2+}]_i$ and trigger exocytosis in bovine chromaffin cells. In addition, depolarization-evoked exocytosis is strongly facilitated when the current is activated.

Tg and BAPTA activate similar Ca^{2+}- and Na^+-carrying currents

Application of the SERCA pump inhibitor Tg or intracellular perfusion with the Ca^{2+} chelator BAPTA evoked transient inward currents at negative holding potentials. Both I_{Tg} and I_{BAPTA} developed and inactivated slowly over several minutes and had similar average maximal amplitude, ion selectivity, and linear *I–V* relationship between −120 and −60 mV. I_{Tg} and I_{BAPTA} share some properties with I_{CRAC}, including receptor-free activation by depletion of intracellular stores, Ca^{2+} permeability, and block by Zn^{2+} (Hoth and Penner, 1993; Lewis and Cahalan, 1995; Parekh and Penner, 1997). Because Tg and BAPTA have different mechanisms of action but share the property of decreasing the Ca^{2+} content of intracellular stores (Hoth and Penner, 1992), we con-

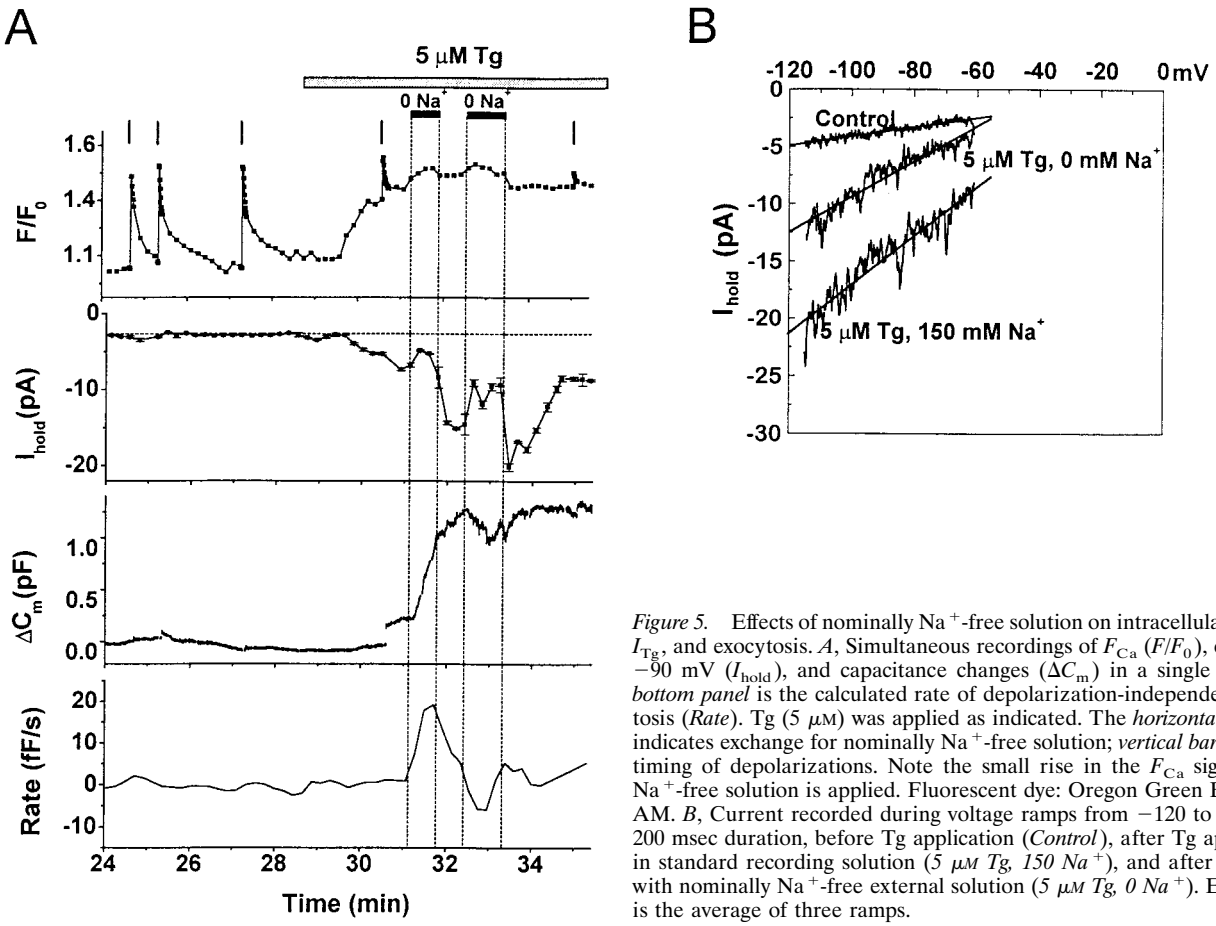

Figure 5. Effects of nominally Na^+-free solution on intracellular $[Ca^{2+}]$, I_{Tg}, and exocytosis. *A*, Simultaneous recordings of F_{Ca} (F/F_0), current at −90 mV (I_{hold}), and capacitance changes (ΔC_m) in a single cell. The *bottom panel* is the calculated rate of depolarization-independent exocytosis (*Rate*). Tg (5 μM) was applied as indicated. The *horizontal dark bar* indicates exchange for nominally Na^+-free solution; *vertical bars* indicate timing of depolarizations. Note the small rise in the F_{Ca} signal when Na^+-free solution is applied. Fluorescent dye: Oregon Green BAPTA-1 AM. *B*, Current recorded during voltage ramps from −120 to −60 mV, 200 msec duration, before Tg application (*Control*), after Tg application in standard recording solution (*5 μM Tg, 150 Na+*), and after exchange with nominally Na^+-free external solution (*5 μM Tg, 0 Na+*). Each trace is the average of three ramps.

clude that I_{Tg} and I_{BAPTA} in chromaffin cells are members of the family of SOCs.

Our experiments eliminate several alternative activation mechanisms for these currents. I_{Tg} and I_{BAPTA} are not Ca^{2+}-activated currents, because depolarizing pulses evoked large-amplitude Ca^{2+} currents and a rapid rise in F_{Ca} that was sustained for several tens of seconds but was never accompanied by an additional inward current. Also, an inward current developed in 10 mM BAPTA, and subsequent application of Tg reactivated a similar current, although high concentrations of a Ca^{2+} chelator with rapid binding kinetics prevent opening of Ca^{2+}-operated channels (Marty and Neher, 1985; Roberts, 1993). Neither I_{Tg} nor I_{BAPTA} are caused by insertion of channel-containing membrane, because all exocytosis was abolished in cells perfused with 10 mM BAPTA. I_{Tg} and I_{BAPTA} are not caused by nonspecific interactions of Tg or BAPTA with the plasma membrane, because both currents are transient in the continuous presence of either compound.

The SOCs described here are not as highly Ca^{2+} selective as I_{CRAC}. Removal of extracellular Na^+ decreased the amplitude of I_{Tg} by 58%, suggesting a relatively high permeability for Na^+. However, Na^+ removal consistently produced a concurrent rise in $[Ca^{2+}]_i$. In intact chromaffin cells, Na^+-free solutions cause elevation of $[Ca^{2+}]_i$ because of the reversal of the plasma membrane Na–Ca exchanger (Chern et al., 1992; Pan and Kao, 1997). In our standard experimental conditions, the Na–Ca exchanger should function in forward mode at negative holding potentials. Because the exchanger is electrogenic, a component of I_{Tg} may consist of Na–Ca exchanger current. A more accurate measure of the ion selectivity was obtained for I_{BAPTA}, because activation of the Na–Ca exchanger is prevented by high concentrations of Ca^{2+} chelators (Hilgemann, 1990). I_{BAPTA} was reduced by only 26% in Na^+-free solution, consistent with the hypothesis that I_{Tg} has both store-operated and Na–Ca exchanger current components. The combined results suggest that the Ca^{2+}–Na^+ selectivity of the SOCs in chromaffin cells is comparable to, or higher than, other SOCs described previously in MDCK cells (Delles et al., 1995) and in cells expressing the insect *trp* gene product channel (Vaca et al., 1994).

There are several unresolved issues concerning both the ion selectivity and kinetics of I_{Tg} and I_{BAPTA}. The *I–V* relationships of these currents were determined between −120 to −60 mV to avoid activation of voltage-gated currents. Linear extrapolation of the *I–V* plot yielded an unexpectedly negative reversal potential. A possible explanation is that the *I–V* relationship is nonlinear over a broad potential range. Indeed, the *I–V* plot for I_{CRAC} exhibits strong curvature, with inward rectification at negative potentials and reversal at positive membrane potentials (Hoth and Penner, 1992; Kerschbaum and Cahalan, 1998).

Another difficulty is that the currents recorded at negative holding potentials may be contaminated by undetermined "leak" conductances in addition to the Na–Ca exchanger current. These may account for the reduction of I_{Tg} to below prestimulatory levels in low-Ca^{2+}, Na^+-free solution, and the incomplete inhibition of I_{BAPTA} in nominally Ca^{2+}- and Na^+-free external solution. Alternatively, the ionic composition of solutions may have direct regulatory effects on the currents. Several previous studies have demonstrated that extracellular and intracellular

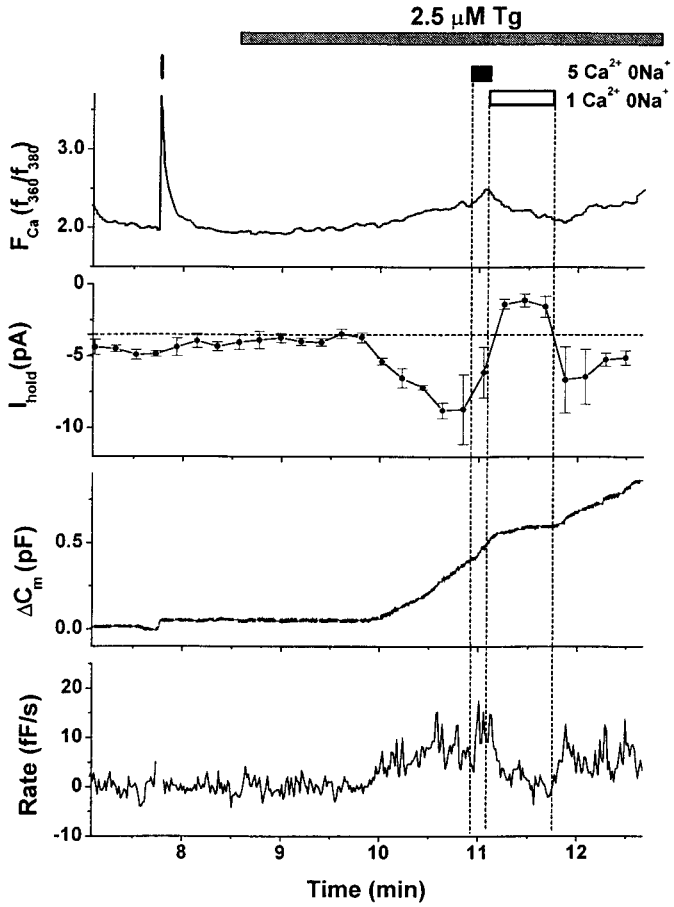

Figure 6. Effects of Na^+-free, low-Ca^{2+} extracellular solution on the thapsigargin-induced changes in intracellular $[Ca^{2+}]$, I_{Tg}, and exocytosis. Plots are of ratio of fura-2 AM fluorescence at 360 and 380 nM excitation wavelengths (F_{Ca}), current at −90 mV (I_{hold}), and capacitance changes (ΔC_m) in a single cell. The *bottom panel* is the calculated rate of depolarization-independent exocytosis (*Rate*). Tg (2.5 μM) was applied as indicated. The *horizontal dark bars* indicate exchange first for nominally Na^+-free solution with 5 mM Ca^{2+}, then for Na^+-free solution with 1 mM Ca^{2+}. *Vertical bar* indicates timing of depolarization.

divalent cation binding sites modulate the kinetics and ion selectivity of SOCs in nonexcitable cells (Delles et al., 1995; Christian et al., 1996; Zweifach and Lewis, 1996; Kerschbaum and Cahalan, 1998).

Finally, the kinetic properties of SOCs are complex (for review, see Parekh and Penner, 1997). SOCs are regulated by numerous factors, including the degree and rate of store depletion (Fasolato et al., 1998; Hofer et al., 1998), second messengers such as protein kinase C (Parekh and Penner, 1995), and Ca^{2+} passage through the CRAC channel (Zweifach and Lewis, 1995a,b; Parekh, 1998). Multiple regulatory mechanisms may account for the complex time course and activation and inactivation properties of I_{Tg} and I_{BAPTA}. Further work is required to fully characterize the properties of the SOCs in bovine chromaffin cells.

The results presented here contradict the conclusion of a previous brief report that Tg or Ca^{2+} chelators do not induce depletion-activated Ca^{2+} currents in bovine chromaffin cells (Bodding and Penner, 1996). There are three major differences in experimental conditions that may account for the discrepancy: (1) our use of perforated-patch instead of whole-cell recording for all Tg experiments; (2) inclusion of 10 mM BAPTA rather than 10–20 mM EGTA in whole-cell recordings; and (3) recording at higher temperature. Because of the complex, poorly understood regulation of SOCs, activation may require specific experimental conditions that were not met in the previous study.

Ca^{2+} influx via a store-operated current can trigger and facilitate exocytosis in bovine chromaffin cells

Although the SOC in bovine chromaffin cells requires further characterization, the key finding of the present study is that store-operated Ca^{2+} influx may have profound effects on exocytosis in excitable cells. A possible modulatory role of capacitative Ca^{2+} entry on exocytosis in chromaffin cells has been suggested based on experiments that did not control for other pathways of Ca^{2+} influx (Powis et al., 1996). Here we demonstrate directly that receptor-free activation of a SOC is sufficient to trigger and/or facilitate exocytosis in bovine chromaffin cells.

In agreement with previous observations (Cheek and Thastrup, 1989), we found that Tg application stimulates the appearance of the intraluminal enzyme DβH on the cell surface of intact cells within 2 min, which corresponds to the onset of depolarization-independent capacitance increases in voltage-clamped cells. This suggests that the capacitance increases observed after store depletion reflect exocytosis of catecholamine-containing large dense-cored vesicles.

Several lines of evidence indicate that depolarization-independent exocytosis at negative potentials is caused by Ca^{2+} influx through I_{Tg}. Exocytosis ceased when extracellular Ca^{2+} was lowered or when I_{Tg} was blocked by extracellular application of Zn^{2+}, an inorganic inhibitor of SOCs in nonexcitable cells (Hoth and Penner, 1993; Zhang and McCloskey, 1995). Depolarization-independent exocytosis was never seen when lower concentrations of Tg evoked a smaller amplitude inward current that was insufficient to increase the $[Ca^{2+}]_i$. Even very high Tg concentrations did not evoke I_{Tg} or trigger exocytosis when applied in an extracellular solution containing low Ca^{2+}.

Facilitation of depolarization-evoked exocytosis was observed in all cells with a Tg-activated current. In cells with detectable $[Ca^{2+}]_i$ elevation, the Ca^{2+} efficacy in evoking exocytosis ($\Delta C_m/Q_{Ca}$) rose and declined in parallel with I_{Tg} and the F_{Ca} signal. In cells without measurable $[Ca^{2+}]_i$ elevation, I_{Tg} and facilitation were sustained for up to 20–25 min. The parallel time course and magnitude of the inward current and facilitation strongly suggests that Ca^{2+} influx through I_{Tg} is responsible for facilitation.

The amplitude of I_{Tg} is approximately 50- to 100-fold less than that of voltage-gated Ca^{2+} currents in bovine chromaffin cells. The ability of a SOC to trigger or facilitate Ca^{2+}-dependent exocytosis in chromaffin cells probably is caused by its prolonged activation. During single depolarizing pulses, exocytosis in these cells is initiated within milliseconds and can proceed at rates as high as 500–1000 fF/sec (Augustine and Neher, 1992). Tg-induced depolarization-independent exocytosis occurs at slow rates (~17 fF/s) and with a significant delay (~45 sec) after activation of I_{Tg} and elevation of F_{Ca}. Despite the slow rate, the total membrane addition was substantial (~1000 fF; range, 500–2000 fF), representing the fusion of ~300–400 large dense-cored vesicles (assuming ~2.5–3 fF/vesicle) (Plattner et al., 1997). This considerably exceeds the predicted size of the release-ready vesicle pool in chromaffin cells (Gillis et al., 1996). Sustained Ca^{2+} influx may saturate Ca^{2+} binding sites and buffers, eventually resulting in substantial local Ca^{2+} elevation. Additionally, prolonged Ca^{2+} influx will probably cause changes in the Ca^{2+} dependence of exocytosis by priming vesicles or the secretory

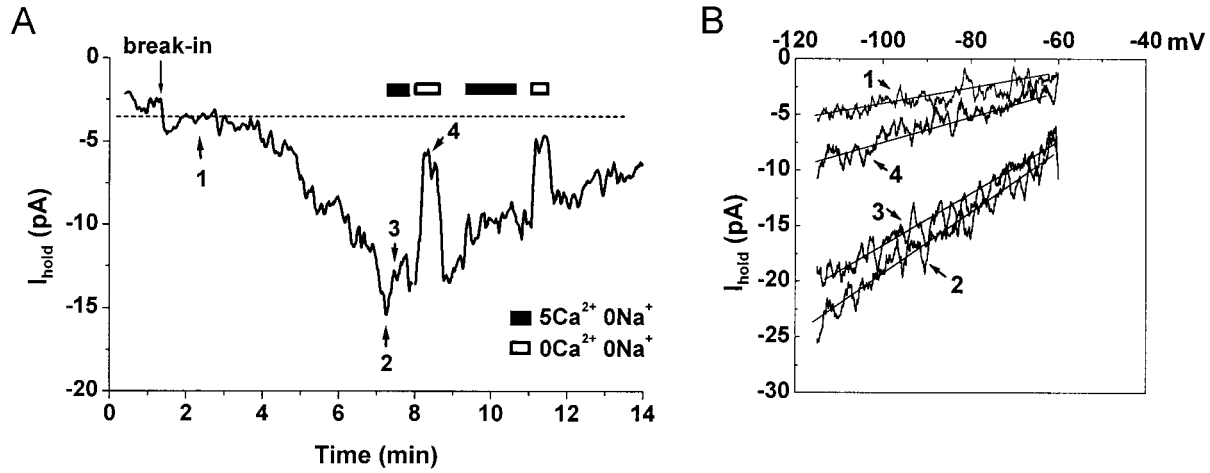

Figure 7. Current activated by intracellular perfusion with 10 mM BAPTA. *A*, Holding current recorded at −90 mV in whole-cell configuration. The patch pipette contained 10 mM BAPTA. *break-in* indicates moment of membrane rupture. *Horizontal bars* indicate exchange of external solution from the standard (5 mM Ca^{2+}, 150 mM Na^+), to Na^+-free solution (5 mM Ca^{2+}, 150 mM $NMDG^+$), to a solution that contained no added Ca^{2+} or Na^+ (0 Ca^{2+}, 150 mM $NMDG^+$). *Numbered arrows* indicate timing of voltage ramps shown in *B*. *B*, Currents recorded during voltage ramps from −120 to −60 mV, 200 msec duration acquired just after *break-in* (*1*), at maximum development of an inward current (*2*), in Na^+-free, but Ca^{2+}-containing solution (*3*), and in nominally Na^+- and Ca^{2+}-free solution (*4*).

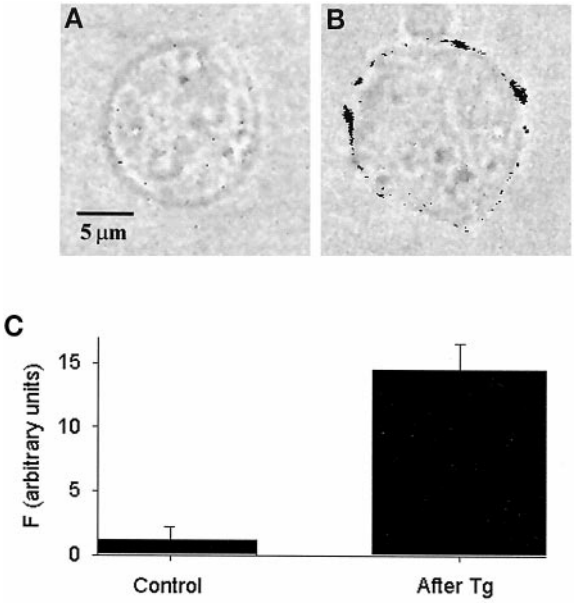

Figure 8. Thapsigargin stimulates exocytosis of catecholamine-containing large dense-cored vesicles. *A*, *B*, Images of chromaffin cells in transmitted light superimposed with inverted fluorescent images of DβH immunofluorescence of the same cells. *A*, Unstimulated control; *B*, cell stimulated with 5 μM Tg for 2 min. DβH immunofluorescent staining appears as a *ring of black patches* on the surface of Tg-stimulated cell. *C*, Mean fluorescent intensity (*F*) of confocal images of nonstimulated cells (*Control*, $n = 11$) and Tg-stimulated cells (*After Tg*, $n = 11$). Background fluorescence was not subtracted. The two groups are significantly different ($p < 0.001$, Student's *t* test).

machinery, possibly via activation of second messengers or Ca^{2+}-dependent cytoskeletal rearrangements (Cheek and Burgoyne, 1991; Heinemann et al., 1993; Vitale et al., 1995; Gillis et al., 1996).

In excitable cells, store-operated Ca^{2+}-permeable currents may be activated by stimulation of IP_3-linked receptors. Hyperpolarization, which is often associated with receptor stimulation (Artalejo et al., 1993), would amplify Ca^{2+} influx via SOCs. This influx, possibly combined with Ca^{2+} released from intracellular stores, may be sufficient to trigger exocytosis at negative holding potentials. Under physiological conditions, cation influx may also contribute to subsequent depolarization and opening of voltage-gated Ca^{2+} channels (Luthi and McCormick, 1998). Finally, Ca^{2+} influx through SOCs may facilitate exocytosis induced by bursts of action potentials. Thus, SOCs in excitable cells may underlie several forms of long-lasting modulation of stimulus-secretion coupling.

REFERENCES

Armstrong CM, Lopez-Barneo J (1987) External calcium ions are required for potassium channel gating in squid neurons. Science 236:712–714.

Artalejo AR, Garcia AG, Neher E (1993) Small-conductance Ca^{2+}-activated K^+ channels in bovine chromaffin cells. Pflügers Arch 423:97–103.

Augustine GJ, Neher E (1992) Calcium requirement for secretion in bovine chromaffin cells. J Physiol (Lond) 450:247–271.

Augustine GJ, Charlton MP, Smith SJ (1987) Calcium action in synaptic transmitter release. Annu Rev Neurosci 10:633–693.

Berridge MJ (1995) Capacitative calcium entry. Biochem J 312:1–11.

Berridge MJ (1998) Neuronal calcium signalling. Neuron 21:13–26.

Bödding M, Penner R (1996) Do chromaffin cells have capacitative Ca^{2+} influx? Biophys J 70:A318.

Burgoyne RD (1991) Control of exocytosis in adrenal chromaffin cells. Biochem Biophys Acta 1071:174–202.

Buryi V, Morel N, Salomone S, Kerger S, Godfraind T (1995) Evidence for a direct interaction of thapsigargin with voltage-dependent Ca^{2+} channel. Naunyn Schmiedebergs Arch Pharmacol 351:40–45.

Cheek TR, Thastrup O (1989) Internal Ca^{2+} mobilization and secretion in bovine adrenal chromaffin cells. Cell Calcium 10:213–221.

Cheek TR, Burgoyne RD (1991) Cytoskeleton in secretion and neurotransmitter release. In: The neuronal cytoskeleton (Burgoyne RE, ed), pp 309–325. New York: Wiley-Liss.

Chern Y-J, Chueh S-H, Lin Y-J, Ho C-M, Kao L-S (1992) Presence of Na^+/Ca^{2+} exchange activity and its role in regulation of intracellular calcium concentration in bovine adrenal chromaffin cells. Cell Calcium 13:99–106.

Chow R, von Ruden L, Neher E (1992) Delay in vesicle fusion revealed by electrochemical monitoring of single secretory events in adrenal chromaffin cells. Nature 356:60–63.

Christian EP, Spence KT, Togo JA, Dargis PG, Patel J (1996) Calcium-dependent enhancement of depletion-activated calcium current in Jurkat T lymphocytes. J Membr Biol 150:63–71.

Clapham DE (1995) Calcium signaling. Cell 80:259–268.
Delles C, Haller T, Dietl P (1995) A highly calcium-selective cation current activated by intracellular calcium release in MDCK cells. J Physiol (Lond) 486:557–569.
Dolmetsch RE, Xu,K, Lewis RS (1998) Calcium oscillations increase the efficiency and specificity of gene expression. Nature 392:933–936.
Douglas WW, Rubin RP (1963) The mechanism of catecholamine release from the adrenal medulla and the role of calcium in stimulus-secretion coupling. J Physiol (Lond) 167:288–319.
Dromaretsky AA, Kabanchenko SI, Fomina AF (1997) Fast spatially resolved fluorescent measurements with multipoint imaging photometer. Biophys J 72:A213.
Engisch KL, Nowycky MC (1996) Calcium dependence of large dense-cored vesicle exocytosis evoked by calcium influx in bovine adrenal chromaffin cells. J Neurosci 16:1359–1369.
Engisch KL, Nowycky MC (1998) Evidence for two types of endocytosis following single step depolarizations in bovine adrenal chromaffin cells. J Physiol (Lond) 506:591–608.
Fanger CM, Hoth M, Crabtree GR, Lewis RS (1995) Characterization of T cell mutants with defects in capacitative calcium entry: genetic evidence for the physiological roles of CRAC channels. J Cell Biol 113:1–13.
Fasolato C, Innocenti B, Pozzan T (1994) Receptor activated Ca^{2+} influx: how many mechanisms for how many channels? Trends Pharmacol Sci 15:77–83.
Fasolato C, Pizzo P, Pozzan T (1998) Delayed activation of the store-operated calcium current induced by calreticulin overexpression in RBL-1 cells. Mol Biol Cell 9:1513–1522.
Fidler N, Fernandez JM (1989) Phase tracking: an improved phase detection technique for cell membrane capacitance measurements. Biophys J 56:1153–1162.
Fomina A, Levitan ES (1995) Three phases of TRH-induced facilitation of exocytosis by single lactotrophs. J Neurosci 15:4982–4991.
Gillis KD, Mossner R, Neher E (1996) Protein kinase C enhances exocytosis from chromaffin cells by increasing the size of the readily releasable pool of secretory granules. Neuron 16:1209–1220.
Gray R, Rajan AS, Radcliffe KA, Yakehiro M, Dani JA (1996) Hippocampal synaptic transmission enhanced by low concentrations of nicotine. Nature 383:713–716.
Heinemann C, von Ruden L, Chow RH, Neher E (1993) A two-step model of secretion control in neuroendocrine cells. Eur J Physiol 424:105–112.
Hilgemann DW (1990) Regulation and deregulation of cardiac Na^+-Ca^{2+} exchange in giant excised sarcolemmal membrane patches. Nature 344:242–245.
Hofer AM, Fasolato C, Pozzan T (1998) Capacitative Ca^{2+} entry is closely linked to the filling state of internal Ca^{2+} stores: a study using simultaneous measurements of I_{CRAC} and intraluminal [Ca^{2+}]. J Cell Biol 140:325–334.
Horrigan FT, Bookman RJ (1994) Releasable pools and the kinetics of exocytosis in adrenal chromaffin cells. Neuron 13:1119–1129.
Hoth M, Penner R (1992) Depletion of intracellular calcium stores activates a calcium current in mast cells. Nature 355:353–356.
Hoth M, Penner R (1993) Calcium release-activated calcium current in rat mast cells. J Physiol (Lond) 465:359–386.
Joshi C, Fernandez JM (1988) Capacitance measurements. An analysis of the phase detection technique used to study exocytosis and endocytosis. Biophys J 53:885–892.
Katz B (1962) The Croonian Lecture. The transmission of impulses from nerve to muscle and the subcellular unit of synaptic action. Proc R Soc Lond B Biol Sci 155:455–477.
Kerschbaum HH, Cahalan MD (1998) Monovalent permeability, rectification, and ionic block of store-operated calcium channels in Jurkat T lymphocytes. J Gen Physiol 111:521–537.
Lewis RS, Cahalan MD (1989) Mitogen-induced oscillations of cytosolic Ca^{2+} and transmembrane Ca^{2+} current in human leukemic T cells. Cell Regul 1:99–112.
Lewis RS, Cahalan MD (1995) Ca^{2+} and K^+ channels in lymphocytes. Annu Rev Immunol 13:623–652.
Li Y-X, Stojilkovic SS, Keizer J, Rinzel J (1997) Sensing and refilling calcium stores in an excitable cell. Biophys J 72:1080–1091.
Lim NF, Nowycky MC, Bookman RJ (1990) Direct measurement of exocytosis and calcium currents in single vertebrate nerve terminals. Nature 344:449–451.
Liu Y-J, Gylfe E (1997) Store-operated Ca^{2+} entry in insulin-releasing pancreatic β-cells. Cell Calcium 22:277–286.
Luthi A, McCormick DA (1998) H-current: properties of neuronal and network pacemaker. Neuron 21:9–12.
Marty A, Neher E (1985) Potassium channels in cultured bovine adrenal chromaffin cells. J Physiol (Lond) 367:117–141.
Mollard P, Seward EP, Nowycky MC (1995) Activation of nicotinic receptors triggers exocytosis from bovine chromaffin cells in the absence of membrane depolarization. Proc Natl Acad Sci USA 92:3065–3069.
Neher E (1988) The influence of intracellular calcium concentration on degranulation of dialysed mast cells from rat peritoneum. J Physiol (Lond) 395:193–214.
Neher E, Marty A (1982) Discrete changes of cell membrane capacitance observed under conditions of enhanced secretion in bovine adrenal chromaffin cells. Proc Natl Acad Sci USA 79:6712–6716.
Nelson EJ, Li CC-R, Bangalore R, Benson T, Kass RS, Hinkle PM (1994) Inhibition of L-type calcium channel activity by thapsigargin and 2,5-t-butylhydroquinone, but not by cyclopiazonic acid. Biochem J 302:147–154.
Obejero-Paz CA, Jones JW, Scarpa A (1998) Multiple channels mediate calcium leakage in the A7r5 smooth muscle-derived cell line. Biophys J 75:1271–1286.
Pan C-Y, Kao L-S (1997) Catecholamine secretion from bovine adrenal chromaffin cells: the role of the Na^+/Ca^{2+} exchanger and the intracellular Ca^{2+} pool. J Neurochem 69:1085–1095.
Parekh AB (1998) Slow feedback inhibition of calcium release-activated calcium current by calcium entry. J Biol Chem 273:14925–14932.
Parekh AB, Penner R (1995) Depletion activated calcium current is inhibited by protein kinase in RBL-2H3 cells. Proc Natl Acad Sci USA 92:7907–7811.
Parekh AB, Penner R (1997) Store depletion and calcium influx. Physiol Rev 77:901–930.
Penner R, Matthews G, Neher E (1988) Regulation of calcium influx by second messengers in rat mast cells. Nature 334:499–504.
Phillips JH, Burridge K, Wilson SP, Kirshner N (1983) Visualization of the exocytosis/endocytosis secretory cycle in cultured adrenal chromaffin cells. J Cell Biol 97:1906–1917.
Plattner H, Artalejo AR, Neher E (1997) Ultrastructural organization of bovine chromaffin cell cortex: analysis by cryofixation and morphometry of aspects pertinent to exocytosis. J Cell Biol 139:1709–1717.
Powis DA, Clark CL, O'Brien KJ (1996) Depleted internal store-activated Ca^{2+} entry can trigger neurotransmitter release in bovine chromaffin cells. Neurosci Lett 204:165–168.
Putney Jr JW (1986) A model for receptor regulated calcium entry. Cell Calcium 7:1–12.
Putney Jr JW (1990) Capacitative calcium entry revisited. Cell Calcium 11:611–624.
Rae J, Cooper K, Gates G, Watsky M (1991) Low access resistance perforated patch recordings using amphotericin B. J Neurosci Methods 37:15–26.
Roberts WM (1993) Spatial calcium buffering in saccular hair cells. Nature 363:74–76.
Robinson IM, Burgoyne RD (1991) Characterization of distinct inositol 1,4,5-trisphosphate-sensitive and caffeine-sensitive calcium stores in digitonin-permeabilized adrenal chromaffin cells. J Neurochem 56:1587–1593.
Robinson IM, Cheek TR, Burgoyne RD (1992) Ca influx induced by Ca-ATPase inhibitors 2,5-di-(t-butyl)-1,4-benzohydroquinone and thapsigargin in bovine adrenal chromaffin cells. Biochem J 288:457–463.
Robinson IM, Yamada M, Carrion-Vazques M, Lennon VA, Fernandez JM (1996) Specialized release zones in chromaffin cells examined with pulse-laser imaging. Cell Calcium 20:181–201.
Seward EP, Chernevskaya NI, Nowycky MC (1995) Exocytosis in peptidergic nerve terminals exhibits two calcium sensitive phases during pulsatile calcium entry. J Neurosci 15:3390–3399.
Thastrup O, Cullen PJ, Dtrobak BK, Hynley MR, Dawson AP (1990) Thapsigargin, a tumor promoter, discharges intracellular Ca^{2+} stores by specific inhibition of the endoplasmic reticulum Ca^{2+}-ATPase. Proc Natl Acad Sci USA 87:2466–2470.

Tomsig JL, Suszkiw JB (1996) Metal selectivity of exocytosis in α-toxin-permeabilized bovine chromaffin cells. J Neurochem 66:644–650.

Vaca L, Sinkins WG, Hu Y, Kunze DL, Schilling WP (1994) Activation of recombinant *trp* by thapsigargin in Sf9 insect cells. Am J Physiol 267:C1501–C1505.

Villalobos C, Garcia-Sancho J (1995) Capacitative Ca^{2+} entry contributes to the Ca^{2+} influx induced by thyrotropin-releasing hormone (TRH) in GH3 pituitary cells. Pflügers Arch Eur J Physiol 430:923–935.

Vitale ML, del Castillo AR, Tchakarov L, Trifaro J-M (1991) Cortical filamentous actin disassembly and scinderin redistribution during chromaffin cell stimulation precede exocytosis: a phenomenon not exhibited by gelsolin. J Cell Biol 113:1057–1067.

Vitale ML, Seward EP, Trifaro J-M (1995) Chromaffin cell cortical actin network dynamics control the size of the release-ready vesicle pool and the initial rate of exocytosis. Neuron 14:353–363.

Wick PF, Trenkle JM, Holz RW (1997) Punctate appearance of dopamine-β-hydroxylase on the chromaffin cell surface reflects the fusion of individual chromaffin granules upon exocytosis. Neuroscience 80:847–860.

Zerbes M, Bunn SJ, Powis DA (1998) Histamine causes Ca^{2+} entry via both a store-operated and a store-independent pathway in bovine adrenal chromaffin cells. Cell Calcium 23:379–386.

Zhang L, McCloskey MA (1995) Immunoglobulin E receptor-activated calcium conductance in rat mast cells. J Physiol (Lond) 483:59–66.

Zweifach A, Lewis RS (1995a) Rapid inactivation of depletion-activated calcium current (I_{CRAC}) due to local calcium feedback. J Gen Physiol 105:209–226.

Zweifach A, Lewis RS (1995b) Slow calcium-dependent inactivation of depletion-activated calcium current. Store-dependent and -independent mechanisms. J Biol Chem 70:14445–14451.

Zweifach A, Lewis RS (1996) Calcium-dependent potentiation of store-operated calcium channels in T lymphocytes. J Gen Physiol 107: 597–610.